High-Frequency Estimation of Shielding Effectiveness Without Inner Sensor in Reverberation Chambers

Philippe Besnier, Jérôme Sol, Marco Klingler, François Sarrazin

High-Frequency Estimation of Shielding Effectiveness Without Inner Sensor in Reverberation Chambers

Philippe Besnier, *Senior Member, IEEE*, Jérôme Sol, Marco Klingler, and François Sarrazin, *Member, IEEE*

***Abstract*—The purpose of this paper is to present a new method for measuring the shielding effectiveness (SE) of enclosures without the use of an internal sensor. This technique uses a reverberation chamber (RC) and relies on the ability to accurately estimate the Q-factor as a function of frequency under different load conditions using an electromagnetic absorbing material. This material is placed successively in the RC, outside and inside the shielded enclosure under test (EUT). Based on the contrast of the Q-factor estimates, it is possible, in a non-invasive way, to characterize the SE of the EUT, using an energy conservation approach. The dynamic range of measurements is assessed. Experimental results are provided. It validates the principle and confirms the estimated dynamic range.**

***Index Terms*—Reverberation chamber, Shielding modeling and method.**

I. Introduction

THE measurement of the shielding effectiveness (SE) of shielded enclosures has a long history in the EMC field. It is currently based on different methods and standards according to their size and the frequency range of measurement. At high frequencies, i.e. frequencies for which the enclosure size is in the order of magnitude of the wavelength, such measurements are tricky due to intrinsic variations of fields according to positions of antennas(s) or probe(s) both within and outside of the enclosure under test (EUT). Moreover, SE depends on the enclosure contents, specifically in the resonance regime of the EUT. These factors have triggered different works over the past twenty years, aiming at improving measurement procedures along with some changes in the SE definition.

The IEEE 299-2006 standard [1] recommends to perform measurement at different positions and orientations to account for these large variations of field distribution within a cavity at resonance. SE is then considered as the weakest result among all measurements. However, for empty cavities with high Q-factor, the inner probe may sense higher field strength than in the absence of the shield. The effect of enclosure contents was investigated or included as a parameter for SE investigations. Experiments and models have confirmed the key role of contents especially at resonance frequency [2]–[4]. Meanwhile, new theoretical definitions of SE where provided in [5], [6]. These papers introduce two quantities. The first consists in integrating the electric field or the magnetic field in the EUT. It accounts definitely for average fields in the enclosure, a much stable indicator that the field strength at a particular position and polarization. The second quantity is based on the evaluation of spatial derivatives of the electric field components that, according to Maxwell's equations, play a key role regarding induced effects. Alternatively, authors in [4] suggest that SE could be defined based on a set of representative contents, i.e. representative pieces of materials possibly equipped with multiple probes. On a more theoretical basis, [7] suggests the use of the infinitesimal lossy sphere to define the SE as the ratio of the power dissipated in this sphere in absence and presence of the shield. It ends with an SE definition, combining magnetic and electric SE performances. This definition has to be considered as an intrinsic property of the shield box itself without any contents. Interestingly, it reflects a definition of the SE in terms of losses rather than in terms of independently seen magnetic and electric field values.

Regarding average power or energy definition of SE, reverberation chambers (RCs) were also considered already some decades ago to perform SE measurements [8], based on illumination of the shielded box under a set of RC states forming a statistically uniform illumination in the form of the so-called plane wave spectrum. In [9] and [10], authors concluded that measuring the SE of physically small but electrically large cavities (i.e. sufficiently overmoded) can be performed when placed in a large RC. Furthermore, mechanical stirring inside such EUT is not required, frequency stirring (i.e. averaging) being sufficient. Simulations have confirmed that fluctuations of the average response of a single inner probe are lower for electrically large EUTs, but remain significant for EUTs with several apertures and low SE [11]. A solution was proposed and also adapted to electrically small EUTs using a long wire as empirical sensor of the modal field cartography throughout the enclosure volume [12]. A one-antenna method has also been proposed based on the Q-factor evaluation of an EUT when the aperture is covered by a metallic sheet [13]. However, as far as small enclosures are concerned, inserting an adequate probe or antenna is an issue [14]. The case of printed circuit board shield is even more problematic and could be solved using a jig equipped with probes and soldering or clamping the shield to be evaluated [15].

Manuscript created July 20, 2023; revised September 12, 2023; accepted September 28, 2023. This work is supported in part by the European Union through the European Regional Development Fund, in part by the Ministry of Higher Education and Research, in part by the Région Bretagne, in part by the Département d'Ille et Vilaine through the CPER Project SOPHIE/STIC & Ondes and the CPER CyMoCoD, and in part by the French "Agence Nationale de la Recherche" (ANR) under Grant ANR-22-CPJ1-0070-01.

P. Besnier, J. Sol and F. Sarrazin are with Univ Rennes, INSA Rennes, CNRS, IETR-UMR 6164, F-35000 Rennes, France.

M. Klingler is with Stellantis, 78943 Vélizy-Villacoublay, France (e-mail: marco.klingler@stellantis.com).

All measurement methods in the literature involve the settlement of one or more probes, fixed or moved at different positions to be installed inside the EUT to sense the internal electric or magnetic field strength. The induced electric signal at the probe terminal must be sent out of the enclosure through appropriate connection using or not an optoelectronic converter. This may be impractical and may also be considered as a destructive test since machining is required.

A non-destructive approach is proposed in this paper. The proposed method is based on using a passive sensor made of a simple and efficient-enough absorbing piece of material. The frequency bandwidth of the method is only limited by the lowest usable frequency (LUF) of the RC used for measurements. The RC composite Q-factor is measured in three configurations: i) without the absorbing material, ii) with the absorbing material inside the RC but outside of the EUT, and iii) with the absorbing material inside the EUT. The contrast of these Q-factors allows retrieving the SE according to a specific definition within a large frequency range. The theoretical basis of the method together with experimental validation are provided. To the best of our knowledge, such a non-invasive approach for SE measurement of enclosures is experimentally demonstrated for the first time.

According to the existing literature, the absorbing piece of material allows to make direct measurement of dissipated power if illuminated in absence or in presence of the shield. It is by nature a distributed sensor and not localized. It is therefore a solution to compensate for the insufficient information recorded from a point-like probe. Regarding the discussion about intrinsic or content-dependent definition of SE, though it obviously heavily loads the EUT, it only aims at converting the electromagnetic field into Joule effect. It is therefore not made for being representative of any contents of the EUT.

The rest of this paper is organized as follows. Section II provides the theory of this passive approach for SE measurements in an RC whereas Section III investigates the dynamic range of the proposed method. Then, Sections IV and V are dedicated to two different experiments involving two different RCs and EUTs, respectively. Some conclusions are drawn in Section VI.

II. Theory

A. The composite Q-factor and its estimation

1) The RC Q-factor: the composite Q-factor [16], [17] is a quantity that enables to predict the behavior of an RC according to modal density and the probability of excitation of multiple modes. Even more importantly, its estimation also enables to calibrate the field intensity in the chamber associated to a prescribed injected power at the input of a transmitting antenna in the RC or vice-versa.

The RC Q-factor is said to be "composite" (or sometimes "effective") for two main reasons that may be confused with one another. The first reason is that losses may come from different mechanisms, e.g., dissipation in the cavity walls, absorption by loading objects or receiving antennas, and aperture leakage. The second reason is that several modes are combined in the chamber, and the Q-factor of single modes cannot be easily retrieved. As far as RCs are concerned, the usual definition of the composite Q-factor corresponds to the average electromagnetic energy stored in the cavity over all states of the chamber obtained during the stirring process, per unit of time, and divided by the total dissipated power in the chamber at steady state. The steady state is reached once the dissipated power balances the transmitted power in the chamber. The composite Q-factor links the ensemble average energy over different states of the chamber and the overall dissipated power as follows:

$$Q = 2\pi f \frac{\mathbb{E}[W_{\mathrm{E}}]}{\mathbb{E}[P_{\mathrm{d}}]}. \tag{1}$$

This definition of quality factor Q applies to steady-state harmonics fields at frequency f and associated pulsation ω and wavelength λ. The notation $\mathbb{E}$ stands for the expected value. The term W_{E} stands for the electromagnetic energy in the chamber and P_{d} represents the active power consumed in the RC.

2) The Q-factor estimation: The Q-factor estimation can be performed with a set of two identical antennas, each connected to one port of a vector network analyser to perform the measurement of the complex-valued scattering matrix elements. The derivation of the estimation of the Q-factor is recalled here for convenience [18]:

$$Q = \frac{\left\langle \left| S_{21} - \langle S_{21} \rangle \right|^2 \right\rangle Z_0 \omega \epsilon V}{(\lambda^2/8\pi)(1 - |\langle S_{11} \rangle|^2)(1 - |\langle S_{22} \rangle|^2)\eta_1 \eta_2}, \tag{2}$$

where Z_0 may be considered as the free-space impedance associated with each individual plane wave composing the whole spectrum, λ_0 is the wavelength, S_{ij} $(i, j \in 1, 2)$ stands for scattering parameters between ports i and j and η_1, η_2 are efficiencies of each antenna.

B. Q-factor of the RC loaded with an empty shielded enclosure

As a first step, the shielded EUT is installed in the RC in an arbitrary position. The initial Q-factor in these conditions is denoted Q_0 and estimated from (2). It is estimated using N uncorrelated positions of a mechanical stirrer. Moreover, the resulting Q-factor is further averaged over M uncorrelated frequencies. Therefore, this estimation leads to an estimation of Q with a total of $N \times M$ realizations. According to the central limit theorem, the Q-factor estimation behaves as a Gaussian distribution centered around the expected value with a standard deviation $\sigma_Q/\sqrt{N \times M}$, where σ_Q is the standard deviation of the underlying probability density function of the Q-factor. In order to reach an acceptable statistical uncertainty for the Q-factor estimation, the product $N \times M$ must be high enough and typically well beyond 1,000.

C. Q-factor of the RC loaded with an empty shielded enclosure and a piece of absorbing material

Adding a piece of absorbing material in the RC induces a modification of the initial composite Q-factor Q_0 due to

additional losses. Given the hypothesis of independence of the different loss mechanisms, the addition of an object in the RC only changes the distribution of the dissipated power among the different loss mechanisms. Therefore, the Q-factor Q_0 is changed to Q_1:

$$\frac{1}{Q_1} = \frac{1}{Q_0} + \frac{1}{Q_{\text{abs\_out\_EUT}}}. \tag{3}$$

The Q-factor of this piece of absorbing material (or any other absorbing object) immersed in the RC can be defined from (1) [16], [17]:

$$Q_{\text{abs\_out\_EUT}} = \frac{2\pi V}{\lambda} \frac{1}{\sigma_{\text{abs\_out\_EUT}}}. \tag{4}$$

where $\sigma_{\text{abs\_out\_EUT}}$ is the averaged absorbing cross section (AACS) of the object, defined as:

$$\sigma_{\text{abs\_out\_EUT}} = \frac{\mathbb{E}[P_{\text{d\_obj}}]}{\mathbb{E}[S_0]}. \tag{5}$$

Therefore, the AACS of the object represents the expected value of the part $P_{\text{d\_obj}}$ of the total active power P_{d} absorbed by the object given the scalar power density S_0 generated in the RC. In the particular case of an absorbing material with a total surface S_{exp} exposed to the RC diffuse field, its AACS can be approximated as [19], [20]:

$$\sigma_{\text{abs\_out\_EUT}} \approx \langle T \rangle \frac{S_{\text{exp}}}{4}. \tag{6}$$

where T is a transmission coefficient expected to be approaching the ideal value $T = 1$ for a well-designed material. As a result, its associated Q-factor is given by:

$$Q_{\text{abs\_out\_EUT}} \approx \frac{8\pi V}{\lambda} \frac{1}{\langle T \rangle S_{\text{exp}}}. \tag{7}$$

It is important to note that this factor depends on the ratio between the chamber volume and the exposed surface of the absorbing element. It is also proportional to frequency. According to (3), the AACS of the absorber can be retrieved from Q_0 and Q_1 measurements from:

$$\sigma_{\text{abs\_out\_EUT}} = \frac{2\pi V}{\lambda} \left(\frac{1}{Q_1} - \frac{1}{Q_0} \right). \tag{8}$$

This AACS represents the absorbing cross-section of the absorbing material directly exposed to the diffuse field generated in the RC.

D. Q-factor of the RC loaded with a shielded enclosure containing a piece of absorbing material

The piece of absorbing material is now placed inside the shielded enclosure itself. The composite Q-factor Q_2 in this new configuration can be defined as

$$\frac{1}{Q_2} = \frac{1}{Q_0} + \frac{1}{Q_{\text{abs\_in\_EUT}}}. \tag{9}$$

Therefore, a new absorbing cross-section $\sigma_{\text{abs\_in\_EUT}}$ can be estimated from Q_2 such as:

$$\sigma_{\text{abs\_in\_EUT}} = \frac{2\pi V}{\lambda} \left(\frac{1}{Q_2} - \frac{1}{Q_0} \right). \tag{10}$$

E. SE evaluation

The SE can be assessed from the contrast of absorbed power by the piece of absorbing material placed outside of the EUT (but inside the RC) and inside the shielded EUT. Therefore, it can be defined as:

$$SE = \frac{\sigma_{\text{abs\_out\_EUT}}}{\sigma_{\text{abs\_in\_EUT}}} \tag{11}$$

Injecting (8) and (10) into (11), it comes:

$$SE = \frac{(Q_0 - Q_1)\, Q_2}{(Q_0 - Q_2)\, Q_1} \tag{12}$$

Therefore, the SE assessment relies on the evaluation of three composite Q-factors of the RC: (i) without the absorbing material (Q_0), (ii) with the absorbing material inside the RC but outside the EUT (Q_1), and (iii) with the absorbing material inside the EUT (Q_2). According to this definition, if the absorbing material is placed in a transparent EUT, the two AACS should be identical and $SE = 1$. On the contrary, if the EUT is perfectly shielded, $\sigma_{\text{abs\_in\_EUT}}$ tends to zero and SE tends to infinity. However, for obvious reasons, the dynamic range of this measurement is limited and must be carefully examined prior determining measurement configurations.

III. Dynamic Range of the Proposed Non-invasive Shielding Effectiveness Measurement Method

According to (11), the dynamic range of such a measurement is bounded, on the one hand, by the absorption performance of the piece of absorber and, on the other hand, by the ability of measuring very low values of AACS, i.e., low values of $\sigma_{\text{abs\_in\_EUT}}$ for well-shielded EUTs. The AACS of the piece of absorbing material should be as high as possible. According to (6), its AACS is proportional to its illuminated external surface (its thickness being supposed larger than the skin depth in the considered frequency range). It should be as large as possible while being limited by the EUT size when placed into it.

Assuming an exponential distribution for Q (with standard deviation $\sigma_Q = 1$), the lowest achievable measurement value of $\sigma_{\text{abs\_in\_EUT}}$ depends on the uncertainty level for the Q-factor estimation. The smallest measurable difference δQ of two Q-factors corresponds to the confidence interval of its estimation:

$$\delta Q = \frac{k}{\sqrt{M_{\text{eff}} N_{\text{eff}}}} \tag{13}$$

where M_{eff} and N_{eff} are the effective size associated to measurements performed with M stirrer positions and N averaging frequencies, respectively, whereas k is a scalar value chosen to correspond to the confidence level choice. At a confidence level of 95% and 99%, $k = 1.96$ and $k = 2.575$, respectively, for a Gaussian distribution. Thus, the minimum deviation of Q_2 from Q_0 writes:

$$Q_2 = (1 - \delta Q) Q_0 \tag{14}$$

Therefore, from (10) and assuming $\delta Q \ll 1$, we easily derive the following result for the minimum achievable AACS if the piece of absorbing material is placed in the EUT:

$$\sigma_{\text{abs\_in\_EUT}_{\min}} = \frac{2\pi V}{\lambda} \frac{\delta Q}{Q_0} \tag{15}$$

The maximum measurable SE ($SE_{\max}$) is then given from:

$$SE_{\max} \approx \langle T \rangle \frac{S_{\text{exp}}}{4} \frac{Q_0 \lambda}{2\pi V} \frac{1}{\delta Q} = \langle T \rangle \frac{S_{\text{exp}}}{4} \frac{Q_0 \lambda}{2\pi V} \frac{\sqrt{M_{\text{eff}} N_{\text{eff}}}}{k} \tag{16}$$

It turns out that increasing the dynamic range may be achieved in two ways. The first one consists in increasing the number of stirrer positions M and averaging uncorrelated frequencies N for Q estimation. The second one consists in testing simultaneously several units of the same EUT, each one associated with its own piece of absorbing material. $SE_{\max}$ is then proportional to the number of simultaneously measured units.

According to (7), a small volume EUT (correspondingly small S_{exp}) in a larger RC would lead to higher $Q_{\text{abs\_out\_EUT}}$ values that would not compensate for the corresponding increase of Q_0 which is also proportional to V but inversely proportional to the RC surface S_{RC}. Therefore, for small EUTs and large RCs, Q_0, Q_1 and obviously Q_2 would become less distinct from each other although large RCs could provide an increasing number of states (i.e. larger M_{eff} and N_{eff}). In other words, without accounting for the possible increase of M_{eff} or N_{eff}, the dynamic range provided in (16) is proportional to the ratio of $S_{\text{exp}}/S_{\text{RC}}$, i.e. losses in the RC walls must not be too large with respect to that of the piece of absorbing material. Still, the used RC must be large enough to operate as a well-stirred RC in the considered frequency range.

IV. Experiment #1 (up to 18 GHz)

A. Experimental Setup

This first experiment takes place in an RC of size $1.75 \times 1.50 \times 2.00$ m^3 (volume of 5.25 m^3) equipped with two rotating mode stirrers (one horizontal and one vertical) made of 4 Z-fold shape paddles (Fig. 1). The RC lowest usable frequency (LUF) is estimated to be around 600 MHz. The considered EUT is an aluminum box of size $42.5 \times 38.8 \times 19.6$ cm^3. The lid of the box is screwed to the base of the box by a series of screws at regular intervals of 5 cm. Thus, the main leakage is supposed to be caused by a set of 6 square apertures of 3 cm arranged in the center of the upper wall. Three identical EUTs are used in this experiment in order to increase the dynamic range of the measurement. Two double-ridged guide horn antennas (ETS-Lindgren Model 3115) are placed on masts within the chamber and connected to two ports of a vector network analyzer (VNA) (Keysight P5024B) in order to measure their scattering parameters. Measurements are performed over the frequency range from 1 GHz to 18 GHz with a 200 kHz frequency step (85001 frequency points). The pieces of absorbing material used are of type Hyfral P150. Their average transmission coefficient $\langle T \rangle$ was determined from their intrinsic properties over the frequency range of 2 GHz to 3 GHz [21]. It is supposed here to be approximately constant over the measurement frequency range and equal to 0.8. Each piece of absorbing material is of size $0.42 \times 0.38 \times 0.10$ m^3. All parameters are recalled in Tab. I.

B. Q-factor Estimation

According to (12), the SE estimation requires a Q-factor measurement for three different configurations:

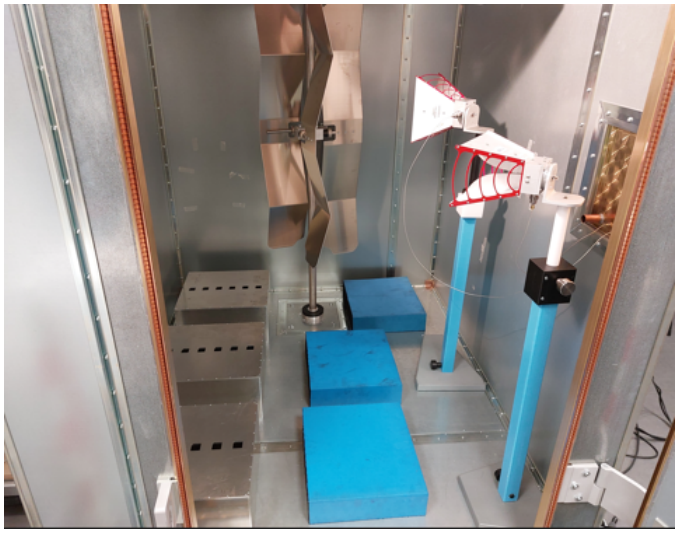

Fig. 1. Photograph of Experiment #1 where three copies of the same EUT as well as three identical pieces of absorbing material are installed in the $1.75 \times 1.50 \times 2.00$ m^3 RC of IETR. Two horn antennas are placed on masts in order to measure the scattering parameters. The test configuration shown corresponds to the estimation of $\sigma_{\text{abs\_out\_EUT}}$ (Q_1).

TABLE I
Experimental properties

Property	Experiment #1	Experiment #2
RC size	$1.75 \times 1.50 \times 2.00$ m^3	$0.580 \times 0.592 \times 0.595$ m^3
EUT size	$42.5 \times 38.8 \times 19.6$ cm^3	$18.3 \times 11.6 \times 4.8$ cm^3
Frequency range	1 GHz to 18 GHz	6 GHz to 30 GHz
Frequency step	200 kHz	400 kHz
Antennas	ETS-Lindgren 3115	RF-Spin DRH 67a
Absorber type	Hyfral P150	
Absorber size	$42 \times 38 \times 10$ cm^3	$18 \times 11 \times 4$ cm^3
Frequency stirring	$N = 1000$	
Mechanical stirring	$M = 30$	

- Step 1: Estimation of the Q-factor Q_0 of the RC loaded with the EUTs alone, without any absorbers.
- Step 2: Estimation of the Q-factor Q_1 of the RC loaded with the EUTs and absorbers located outside of the EUTs, i.e., lying on the RC floor.
- Step 3: Estimation of the Q-factor Q_2 of the RC loaded with the EUTs in which the absorbers have been placed.

Q-factor estimations are performed based on (2) using a frequency averaging ($N = 1000$, i.e., an overall bandwidth of 200 MHz) of ensemble averages obtained from $M = 30$ stirrer positions (two stirrers are moved). The Q-factors Q_0, Q_1 and Q_2 are compared in Fig. 2. Q_1 is significantly lower than Q_0 over the entire frequency range. as expected. Indeed, the presence of the absorbers within the RC drastically increases the losses. However, the estimated Q_2 (once the absorbers are placed inside the EUTs) is much closer to Q_0. These are not distinct from each other below 3 GHz but the absorption due to the absorbers placed inside the EUTs is clearly evidenced above this frequency.

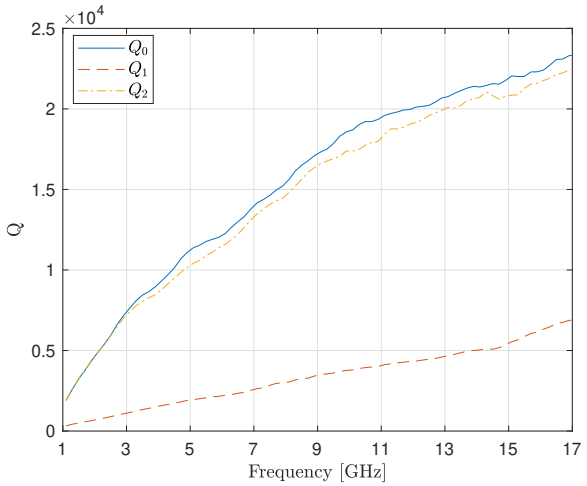

Fig. 2. Q_0, Q_1 and Q_2 estimations for the large RC loaded by the three shielded boxes as a function of frequency (Experiment #1).

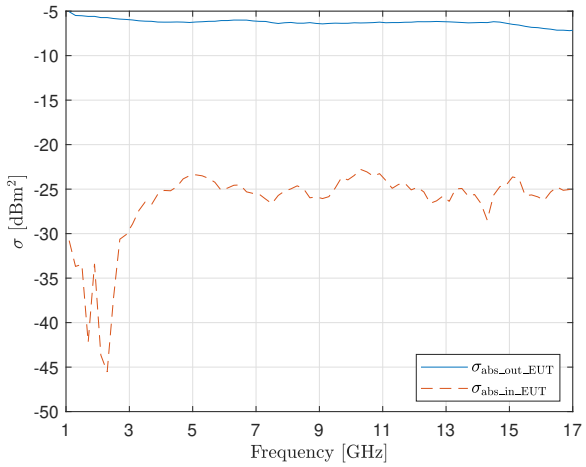

Fig. 3. AACS of the set of the 3 absorbers while inside and outside of the large EUT as a function of frequency (Experiment #1).

C. Dynamic range

The dynamic range is provided from (16) where an approximation of $SE_{\max}$ can be derived from Q_0. The RC volume is 5.250 m^3 and Q_0 is about 17000 at 9 GHz (Fig. 2). As a result, the coherence bandwidth is about 500 kHz. A rough estimation is $N_{\text{eff}} = 400$ over a 200 MHz bandwidth. All stirrer positions are supposed to provide independent realizations: $M_{\text{eff}} = 30$. The 3 pieces of absorbing materials ($\langle T \rangle = 0.8$) lying on the floor are exposed over 5 of their faces. The overall surface $S_{\text{exp}} = 0.3196 \times 3$ m^2. From (16), using a 99% confidence level ($k = 2.575$), we obtain:

$$SE_{\max,\#1} \approx 140 \quad (21.5 \text{ dB}) \tag{17}$$

This range is limited due to two limiting factors. The first one is the limited surface of the pieces of absorbing materials. The second one is related to the limited number of uncorrelated RC states ($M_{\text{eff}} \times N_{\text{eff}}$). Both aspects may be improved but this dynamic range budget is acceptable for the proof of concept introduced in this paper.

D. SE Results

The corresponding AACS $\sigma_{\text{abs\_out\_EUT}}$ and $\sigma_{\text{abs\_in\_EUT}}$ are shown in Fig. 3. It appears that $\sigma_{\text{abs\_in\_EUT}}$ is not significant below 3 GHz and reaches a small but still detectable value above this frequency. According to (15), the detectable AACS is estimated to be 0.0015 m^2 (≈ -28 dBm^2). Apertures are one-tenth of the wavelength at 1 GHz and still appear as small apertures. Absorption is therefore limited in the lowest frequency range and is not detectable due to the limited dynamic range.

The SE results obtained thanks to the measurements of $\sigma_{\text{abs\_out\_EUT}}$ and $\sigma_{\text{abs\_in\_EUT}}$ are compared to a standard SE estimation where a horn antenna is placed inside the EUT. The horn antenna is placed above the absorbing piece of material inside the EUT as shown in Fig. 4. Such a standard measurement could have been done with or without any piece of absorbing material within the EUT. However, as already discussed, resonances in an empty cavity may lead to negative shielding effectiveness, which makes no sense from the energy-conservation point of view. As the method proposed in this paper uses an energy-based definition that aims to be much less dependent on the shape of the cavity and resonance phenomena, we decided to carry out this measurement with a piece of absorbing material in the cavity. Furthermore, the absorbing material was kept identical to maintain the same loss conditions as for the non-invasive measurement. A single EUT is used and equipped with a pass-through connector. The SE is then measured as the ratio of the average power collected in the RC and in the shielded box. The results of the present method and of this standard measurement are highlighted in Fig. 5. However, this standard SE estimation suffers from the usual drawbacks of invasive SE measurements which are sensitive to antenna location and properties. Furthermore, the average field in the EUT is not measured, the antenna being placed in a single position. This specific antenna was selected due to its large bandwidth and compactness.

From the standard measurement, it can be seen that the SE drops from 60 dB at 1 GHz down to 20 dB at 3 GHz. The non-invasive method also identifies the decrease of SE above 3 GHz but the estimated SE is bounded to about 30 dB due to the limited dynamic range. Above 3 GHz the results are consistent with the standard measurement, the SE being overestimated with respect to the measurement performed with a horn antenna whose apparent directivity remains high in a non-reverberating environment. It was also observed that the apertures are responsible for the leakage. Indeed, when closed by metallic tapes, the SE reaches the dynamic range as also shown in Fig. 5. The resulting curve exhibits erratic fluctuations as soon SE exceeds the dynamic range of 21 dB as estimated above. Experiment #1 confirms the ability of this non-invasive SE measurement concept to mimic the trend of a standard measurement performed with an inner sensor.

V. Experiment #2 (up to 30 GHz)

A. Experimental setup

In this section, we propose a second experimental validation of the non-invasive SE measurement method. This experi-

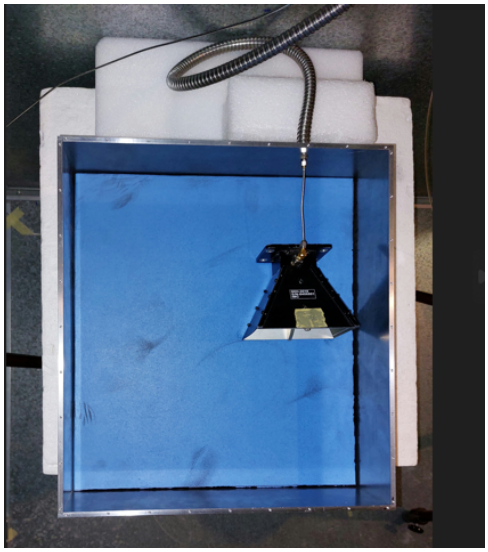

Fig. 4. Picture of the large shielded box equipped with an inner horn antenna for standard SE measurement.

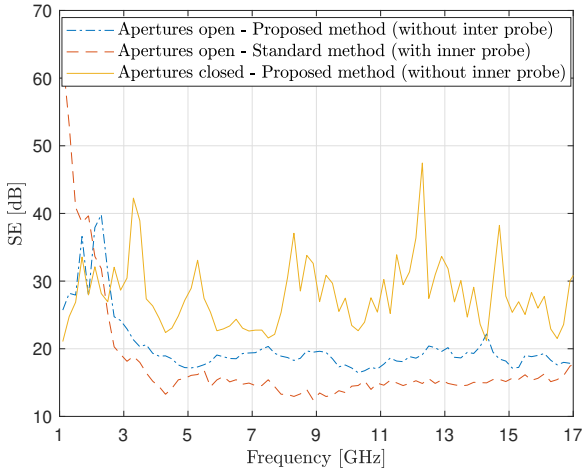

Fig. 5. SE of the large shielded box as a function of frequency estimated with the proposed method and compared to the standard method (Experiment #1). The SE estimated when the EUT apertures are closed is also shown.

ment #2 is performed in a smaller RC of size $0.580 \times 0.592 \times 0.595$ m^3, whose LUF is estimated to be around 2 GHz. Two identical EUTs are placed inside the RC, each of them being an aluminum box of smaller size ($18.3 \times 11.6 \times 4.8$ cm^3) where two circular apertures of diameter of 2 cm are present on both small sides of the box. A picture of the setup is presented in Fig. 6. Two antennas (RF-Spin DRH 67a) are placed within the cavity and connected to a VNA. Measurements are performed over the frequency range from 6 GHz to 30 GHz with a 400 kHz frequency step (60001 frequency points). All parameters are summarised in Tab. I.

B. Q-factor Estimation

The same three-step procedure is followed for this second experiment. The three Q-factor estimations Q_0, Q_1 and Q_2 are compared in Fig. 7. Once again, Q_1 is really small compared to Q_0 due to the high absorption provided by the two large

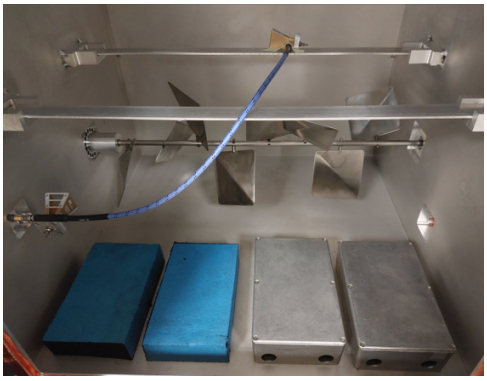

Fig. 6. Photograph of the two copies of the small shielded box #2 installed in the $0.580 \times 0.592 \times 0.595$ m^3 RC of IETR. The test configuration shown corresponds to the estimation of $\sigma_{\text{abs\_out\_EUT}}$ (Q_1).

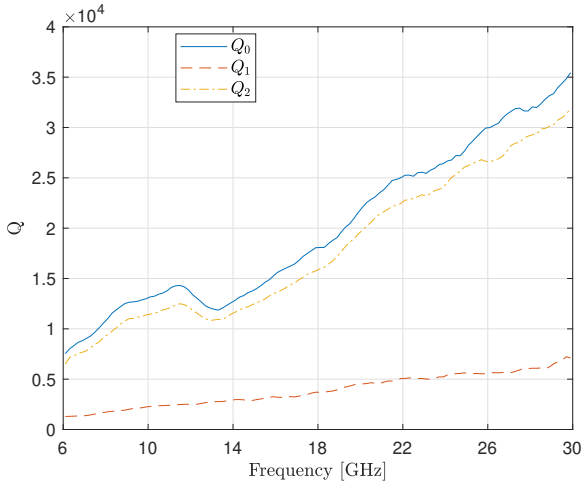

Fig. 7. Q_0, Q_1 and Q_2 estimations for the small RC loaded by the two small shielded boxes as a function of frequency (Experiment #2).

absorbers lying on the RC floor. However, in this experiment, Q_2 is significantly lower than Q_0 over the entire measurement frequency range. Indeed, the cylindrical apertures are not electrically small even in the lowest frequency range, their diameter being close to half of a wavelength at 6 GHz. This explains that absorption is measurable even at the lowest frequency range.

C. Dynamic Range

The RC volume is 0.204 m^3 and Q_0 is about 18000 at the central frequency (18 GHz). As a result, the coherence bandwidth is about 1 MHz and $N_{\text{eff}} = 200$. All stirrer positions are also supposed to provide uncorrelated realizations, i.e., $M_{\text{eff}} = 30$. The 2 pieces of absorbing materials ($\langle T \rangle = 0.8$) lying on the floor are exposed over 5 of their faces. The overall surface $S_{\text{exp}} = 0.043 \times 2$ m^2. From (16), using a 99% confidence level ($k = 2.575$), we obtain:

$$SE_{\text{max},\#2} \approx 120 \quad (20.8 \text{ dB}) \tag{18}$$

D. SE Results

The corresponding AACS $\sigma_{\text{abs\_out\_EUT}}$ and $\sigma_{\text{abs\_in\_EUT}}$ are shown in Fig. 8. When placed in the EUT, the AACS

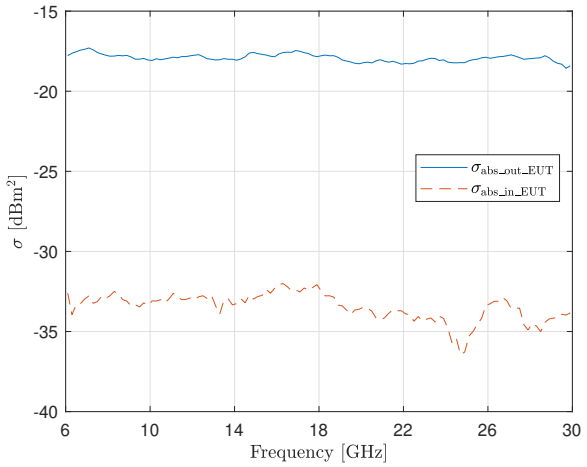

Fig. 8. AACS of the 2 absorbers while inside and outside of the small EUT as a function of frequency (Experiment #2).

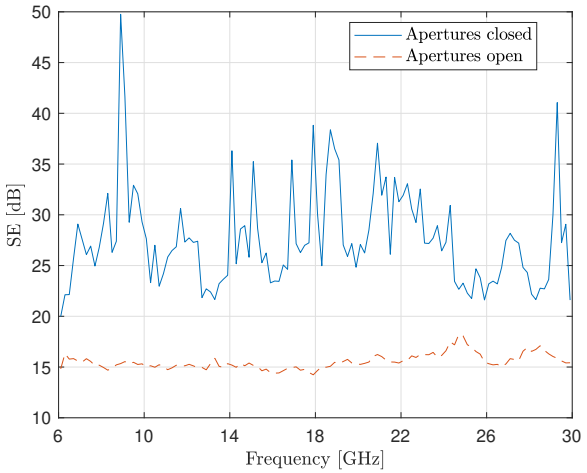

Fig. 9. SE of the small shielded box as a function of frequency (Experiment #2).

of absorbing materials $\sigma_{\text{abs\_in\_EUT}}$ exhibits a nearly constant value over the entire frequency range. According to (15), the detectable AACS is estimated to be 0.00015 m^2, i.e. -38 dBm^2 for this case study which is in the same order of magnitude than the experimental result.

The SE results obtained thanks to the measurements of $\sigma_{\text{abs\_out\_EUT}}$ and $\sigma_{\text{abs\_in\_EUT}}$ are shown in Fig. 9. The estimated SE is close to 15 dB over the entire frequency range. Due to the small size of the EUTs, no standard measurement have been carried out with an inner antenna for this experiment. Results of the present method when the four cylindrical apertures are short-circuited using metallic tapes are also presented in Fig 9. It can be seen that the corresponding SE is higher than 22 dB over the entire frequency range and exhibits erratic fluctuations as a function of frequency which is coherent with the theoretical $SE_{\max,\#2}$ equal to 20.8 dB. It clearly highlights that the four cylindrical apertures are mainly responsible for the leakage.

VI. Conclusion

A novel RC-based SE measurement method has been introduced in this paper. The method is based on the evaluation of the RC composite Q-factor when an absorber is placed successively inside and outside of the shielded EUT located within the RC. The Q-factor contrast allows retrieving the SE of the EUT without the need of any inner probe within the EUT, making this method the first non-invasive approach to perform SE measurements. This method is therefore suitable for SE measurement of shielded box of electronic units or printed circuit board shields.

The method has been validated in a 5.25 m^3 RC in the frequency range from 1 GHz to 18 GHz, where the retrieved SE is similar to the one obtained through a conventional SE measurement method based on the use of an invasive inner probe. A second experiment in a smaller RC (volume of 2 m^3) has confirmed the capability of this method up to 30 GHz.

The measurement dynamic range has been analyzed in order to evaluate the limitation of the current approach. The dynamic range is bounded by the limited absorption provided by the absorbers on the one hand, and by the uncertainty regarding the Q-factor estimation on the other hand. Both experiments that have been presented in this paper exhibit an estimated maximum measurable SE of about 21 dB. The dynamic range can be improved by either increasing the number of uncorrelated RC states, increasing the number of identical EUTs, or using absorbers with higher absorption properties.

References

[1] "IEEE standard method for measuring the effectiveness of electromagnetic shielding enclosures," IEEE Std 299-2006 (Revision of IEEE Std 299-1997), pp. 1–52, 2007.

[2] M. Robinson, T. Benson, C. Christopoulos, J. Dawson, M. Ganley, A. Marvin, S. Porter, and D. Thomas, "Analytical formulation for the shielding effectiveness of enclosures with apertures," IEEE Trans. Electromagn. Compat., vol. 40, no. 3, pp. 240–248, 1998.

[3] F. Olyslager, E. Laermans, D. De Zutter, S. Criel, R. De Smedt, N. Lietaert, and A. De Clercq, "Numerical and experimental study of the shielding effectiveness of a metallic enclosure," IEEE Trans. Electromagn. Compat., vol. 41, no. 3, pp. 202–213, 1999.

[4] A. Marvin, J. Dawson, S. Ward, L. Dawson, J. Clegg, and A. Weissenfeld, "A proposed new definition and measurement of the shielding effect of equipment enclosures," IEEE Trans. Electromagn. Compat., vol. 46, no. 3, pp. 459–468, 2004.

[5] S. Celozzi, "New figures of merit for the characterization of the performance of shielding enclosures," IEEE Trans. Electromagn. Compat., vol. 46, no. 1, pp. 142–, 2004.

[6] R. Araneo and S. Celozzi, "Actual performance of shielding enclosures," in 2004 IEEE Int. Symp. Electromagn. Compat. (IEEE Cat. No.04CH37559), vol. 2, 2004, pp. 539–544 vol.2.

[7] L. Klinkenbusch, "On the shielding effectiveness of enclosures," IEEE Trans. Electromagn. Compat., vol. 47, no. 3, pp. 589–601, 2005.

[8] M. Hatfield, "Shielding effectiveness measurements using mode-stirred chambers: a comparison of two approaches," IEEE Trans. Electromagn. Compat., vol. 30, no. 3, pp. 229–238, 1988.

[9] C. L. Holloway, D. A. Hill, M. Sandroni, J. M. Ladbury, J. Coder, G. Koepke, A. C. Marvin, and Y. He, "Use of reverberation chambers to determine the shielding effectiveness of physically small, electrically large enclosures and cavities," IEEE Trans. Electromagn. Compat., vol. 50, no. 4, pp. 770–782, 2008.

[10] A. C. Marvin and Y. He, "A study of enclosure shielding effectiveness measurement using frequency stirring in a mode-stirred chamber," in 2008 IEEE Int. Symp. Electromagn. Compat., 2008, pp. 1–6.

[11] D. Fedeli, G. Gradoni, V. M. Primiani, and F. Moglie, "Accurate analysis of reverberation field penetration into an equipment-level enclosure," IEEE Trans. Electromagn. Compat., vol. 51, no. 2, pp. 170–180, 2009.

[12] G. B. Tait, C. Hager, M. B. Slocum, and M. O. Hatfield, "On measuring shielding effectiveness of sparsely moded enclosures in a reverberation chamber," IEEE Trans. Electromagn. Compat., vol. 55, no. 2, pp. 231–240, 2013.
[13] Q. Xu, Y. Huang, X. Zhu, L. Xing, Z. Tian, and C. Song, "Shielding effectiveness measurement of an electrically large enclosure using one antenna," IEEE Trans. Electromagn. Compat., vol. 57, no. 6, pp. 1466–1471, 2015.
[14] C. Zhou, L. Gui, and L. Lv, "Shielding effectiveness measurement of small size metal enclosure," in 2016 Asia-Pacific Int. Symp. Electromagn. Compat. (APEMC), vol. 01, 2016, pp. 417–419.
[15] A. C. Marvin and J. F. Dawson, "Efficient measurement techniques and modelling of printed circuit board shields," in 2022 IEEE Int. Symp. Electromagn. Compat., 2022, pp. 47–52.
[16] D. Hill, Electromagnetic fields in cavities: deterministic and statistical theories. IEEE Press Wiley, 2009.
[17] P. Besnier and B. Demoulin, Electromagnetic reverberation chambers. ISTE Wiley & Sons, 2011.
[18] P. Besnier, C. Lemoine, and J. Sol, "Various estimations of composite q-factor with antennas in a reverberation chamber," in 2015 IEEE Int. Symp. Electromagn. Compat., 2015, pp. 1223–1227.
[19] D. Hill, M. Ma, A. Ondrejka, B. Riddle, M. Crawford, and R. Johnk, "Aperture excitation of electrically large, lossy cavities," IEEE Trans. Electromagn. Compat., vol. 36, no. 3, pp. 169–178, 1994.
[20] P. Hallbjorner, U. Carlberg, K. Madsen, and J. Andersson, "Extracting electrical material parameters of electrically large dielectric objects from reverberation chamber measurements of absorption cross section," IEEE Trans. Electromagn. Compat., vol. 47, no. 2, pp. 291–303, 2005.
[21] M. I. Andries, P. Besnier, and C. Lemoine, "On the prediction of the average absorbing cross section of materials from coherence bandwidth measurements in reverberation chamber," in 2012 IEEE Int. Symp. Electromagn. Compat., 2012, pp. 1–6.

Philippe Besnier (M'04, SM'10) received the diplôme d'ingénieur degree in electronics from école universitaire d'ingénieurs de Lille (EUDIL), Lille, France, in 1990 and the Ph. D. degree in electronics from the university of Lille in 1993. Following a one-year period at ONERA, Meudon as an assistant scientist in the EMC division, he was with the laboratory of radio-propagation and electronics (LRPE), university of Lille, as a researcher (chargé de recherche) at the Centre National de la Recherche Scientifique (CNRS) from 1994 to 1997. From 1997 to 2002, Philippe Besnier was the director of Centre d'Etudes et de Recherches en Protection Electromagnétique (CERPEM): a not-for-profit organization for research, expertise and training in EMC and related activities, based in Laval, France. He also co-founded and headed TEKCEM in 1998, a small business company specialized in turn-key systems for EMC measurements. Back to CNRS in 2002, he has been since then with the Institut d'Electronique et des Technologies du numéRique (IETR) - www.ietr.fr -, Rennes, France. Philippe Besnier was appointed as CNRS senior researcher (directeur de recherche au CNRS) in 2013. He was co-head of the "antennas and microwave devices" research department of the IETR between 2012 and 2016. He headed the WAVES (now eWAVES) team - electromagnetic waves in complex media - during the first semester of 2017. Since July 2017, he is deputy director of the IETR. His research activities deal with interference analysis on cable harnesses (including electromagnetic topology), theory and application of reverberation chambers, shielding and absorbing techniques, quantification and propagation of uncertainties in EMC modeling and electromagnetic cybersecurity.

Jérôme Sol photograph and biography not available at the time of publication.

Marco Klingler was born in Zurich, Switzerland, in 1963. He received his Engineer's degree in computer science from HEI, Lille (France) in 1989, his DEA (M.S.) degree in automatics / robotics and his Ph.D. in electronics in 1989 and 1992 respectively, both from the University of Lille. He then joined the French National Institute for Transport and Safety Research (INRETS) in Villeneuve d'Ascq (France) as a researcher where he was in charge of the RD activities in EMC of ground transportation systems. His main interests were electromagnetic interferences on PCBs, behavior of electronic components in electromagnetic environments, coupling to wire structures, test methods, and test facilities. In 2002, he joined Stellantis (former Groupe PSA) in Velizy-Villacoublay (France) in the Development Division where he was successively in charge of the EMC design activities, the EMC / antenna simulation activities, and finally the EMC full vehicle validation activities. In 2011, he moved to the Research Division where he is currently an EMC Expert and responsible of the EMC / antenna research activities. His main interests include EMC modeling and simulation of automotive electric powertrains, multi-conductor transmission lines, new materials, and specific vehicle antennas.

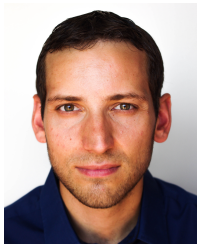

François Sarrazin received the M.S. degree in electronics and electrical engineering from Polytech'Nantes (Ecole polytechnique de l'université de Nantes), France, in 2010, and the Ph.D. degree from the Institut d'Electronique et des Technologies du numéRique (IETR), University of Rennes, France, in 2013. In 2014, he worked as a post-doctorate fellow at the Royal Military College of Canada in Kingston, Ontario. From 2010 to 2014, his research was focused on antenna characterization using the Singularity Expansion Method (SEM) applied both in the time and spatial domains. In 2015, he worked as a research engineer at the CEA-Léti in Grenoble, France, and did his research on electrically-small frequency-agile antenna design and radiation efficiency optimization. From 2016 to 2022, he was an associate professor at Université Gustave Eiffel and ESYCOM laboratory (CNRS UMR 9007). Since September 2022, he hold a "Junior Professor Chair" at University of Rennes and IETR laboratory (CNRS UMR 6164). His research activities include electromagnetic cybersecurity, TEMPEST, reverberation chamber characterization, contactless antenna measurement and antenna radar cross-section measurement.